

Support Vector Machines Based Filtering of Lidar Data: A Grid Based Method

Mahmoud SALAH and John TRINDER, Australia

Key words: Aerial, Lidar, Fusion, Classification, Learning, Filtering.

SUMMARY

This study introduces a method for filtering lidar data based on a Support Vector Machines (SVMs) classification method. Four study areas with different sensors and scene characteristics were investigated. First, the Digital Surface Model (DSM) was generated for the first and last pulses and then the differences between the first and last pulses (FP-LP) were computed. A total of 25 uncorrelated feature attributes have been generated from the aerial images, the lidar intensity image, DSM and FP-LP. The generated attributes were applied in seven separate groups which include those from: Red, Green and Blue bands of the aerial image; Intensity/IR image; DSM; FP-LP and the Total group of attributes. Finally, SVMs were used to automatically classify buildings, trees, roads and ground from aerial images, lidar data and the generated attributes, with the most accurate average classifications of 95% being achieved. The Gaussian Radius Basis Function (RBF) kernel model was applied to find the separating hyperplane for the SVMs classification.

A binary image was then generated by converting the digital numbers of roads and grass to one while the digital numbers of buildings and trees were converted to zeros and all DSM's pixels which correspond to a pixel value of one in the binary image were interpolated into a grid DTM. The interpolated DTM was then smoothed by a low-pass filter to remove low vegetation and other objects which might be classified as ground.

After that the original 3D lidar point clouds was compared against the smoothed DTM and labeled as ground or non-ground based on a predefined threshold of 30 cm.

To meet the objectives, the filtered data was compared against reference data that was generated manually and both omission and commission errors were calculated. Further, we evaluated the contributions of each group of attributes to the quality of the filtering process. The results showed that the accuracy of the results was improved by fusing lidar data with multispectral images regardless of the complexity of the terrain being filtered.

Support Vector Machines Based Filtering of Lidar Data: A Grid Based Method

Mahmoud SALAH and John TRINDER, Australia

1. INTRODUCTION

Lidar has become a reliable technique for data collection of the earth's surface. Because of its characteristics which include acquisition of first and last pulses, penetration of forested areas, narrow field angles, and independence on shadows and object texture, it is considered as the most effective technique for the production of high resolution Digital Terrain Models (DTMs) (Gianfranco and Carla, 2007).

Nowadays the focus of lidar data processing has been on the development of algorithms to extract information from the 3D point cloud, such as terrain information, the extraction of human-made features such as the formation of roads and buildings, and the calculation of forest parameters (Wack and Wimmer, 2002). Many different filtering approaches have been developed to derive highly accurate digital terrain models. For typically non-complex landscapes most of the existing algorithms perform well, but filtering complex urban landscapes still poses the greatest challenges. In this paper, we have suggested using image and lidar data fusion for filtering of complex urban landscapes based on Support Vector Machines (SVM), to assist in understanding the context of the landscape being filtered. This paper is organised as follows. Section 2 reviews related work on the filtering of lidar data. Section 3 describes the study areas and datasets. Section 4 presents the pre-processing of the used data. Section 5 describes the experiments while Section 6 presents and evaluates the results. We summarise our results in Section 7.

2. RELATED WORK

Filtering is the process of separating on-terrain points (DTM) from points falling onto objects such as buildings, cars, trees, and other natural and human made objects. Filtering approaches can be classified in terms of the source of data used into two main approaches: grid based filtering and raw data based filtering.

A considerable number of grid based filtering algorithms have been created to filter lidar data. Firstly a DSM is generated from the lidar point cloud, after which filtering is conducted. Kraus and Pfeifer (1998) filtered lidar data in forest areas using an iterative, linear least squares interpolation method. Vosselman (2000) proposed a filter to remove non-ground measurements by comparing slopes between a lidar point and its neighbours. Okagawa (2001) used a cluster analysis technique to separate ground and non-ground lidar measurements. Haugerud and Harding (2001) employed an algorithm to remove trees in forest areas by comparing local curvatures of point measurements. Passini and Jacobsen (2002) developed a filter approach based on linear prediction of a stationary random function. Elmqvist (2002) classified ground and non-ground measurements based on active contours. Zhang et al.,

(2003) used mathematical morphology to identify non-ground measurements. Mathematical morphology methods suffer various problems such as ineffective removal of various sized non-ground objects due to the requirement of a fixed window size. Zhang and Whitman (2003) proposed an iterative progressive morphological filter to overcome these drawbacks. By gradually increasing the window size and using elevation difference thresholds, the progressive morphological filter removed measurements for different sized non-ground objects while preserving ground data. Gianfranco and Carla (2007) presented a three-stage raw data classification to separate ground and non-ground points.

Alternatively, lidar data can be filtered by selecting ground measurements iteratively from the original data set. Axelsson (2000) developed an adaptive Triangulated Irregular Network (TIN) method to find ground points based on selected seed ground measurements. Whitman et al., (2003) used an elevation threshold and an expanding search window to identify and remove non-ground points. Abo Akel et al. (2004) used a robust method with orthogonal polynomials and road network for automatic terrain surface extraction from lidar data in urban areas. However, the DTM cannot always be generated in areas that do not contain road networks by this method. Also, elevated bridges will be classified as part of the DTM. Bartels (2006) employed wavelets for ground and non-ground points separation from 3D lidar point clouds in hilly terrain.

Sithole and Vosselman (2003) compared the results from eight filtering models against reference data sets. They used models based on: Active Contours; Regularization Method; Modified Slope based filter; Spline interpolation; Hierarchical Modified Block Minimum; Progressive TIN densification; Modified Slope based filter; and Hierarchic robust interpolation. For non-complex landscapes most of the algorithms performed well, while for complex landscapes surface based filters performed better. They suggested using segmentation and data fusion for filtering of complex urban landscapes.

3. STUDY AREA AND DATA SOURCES

Four test data sets of different characteristics and different sizes were used in this study based on SVMs, as shown and summarized in figure 1 and table 1 respectively.

Table 1: Characteristics of image and lidar data sets.

Test area	Size	Lidar Data		Aerial images	
		Sensor	wavelength	bands	pixel size
UNSW	0.5 x 0.5Km	Optech ALTM 1225	1.047 μ m	RGB	10cm
Bathurst	1 x 1Km	Leica ALS50	1.064 μ m	RGB	50cm
Fairfield	2 x 2Km	Optech ALTM 3025	1.047 μ m	RGB	15cm
Memmingen	2 x 2Km	TopoSys	1.56 μ m	CIR	50cm

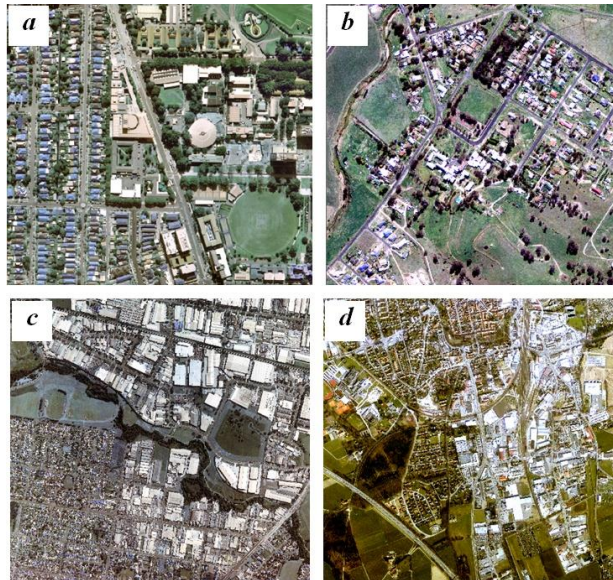


Figure 1: Orthophotos for: (a) UNSW; (b) Bathurst; (c) Fairfield; and (d) Memmingen.

4. DATA PRE-PROCESSING

First, the Digital Surface Model (DSM) was generated for the first and last pulses. Then the differences between the first and last pulses (FP-LP) were computed. Next, a set of 78 possible attributes were selected as shown in Table 2. Because of the way the texture equations derived from the Grey-Level Co-occurrence Matrix (GLCM) (Haralick 1979) are constructed, many of them are strongly correlated with one another (Clausi 2002). Based on these studies, only 25 of the 78 possible attributes were uncorrelated and hence available for the classification process as shown in table 2. The attributes include those derived from the GLCM, Normalized Difference Vegetation Indices (NDVI), slope and the polymorphic texture strength based on the Förstner operator (Förstner and Gülch 1987).

Table 2: ▨ The full set of the attributes; ▩ attributes available for the classification.

Attributes	Attribute	R	G	B	I	DSM	FP-LP
Spectral	Mean	▨	▨	▨	▨	▨	▨
	St. Deviation Strength	▩	▩	▩	▩	▩	▩
GLCM	Contrast	▨	▨	▨	▨	▨	▨
	Dissimilarity	▨	▨	▨	▨	▨	▨
	Homogeneity	▨	▨	▨	▨	▨	▨
	A.S.M	▨	▨	▨	▨	▨	▨
GLCM	Entropy	▨	▨	▨	▨	▨	▨
	Mean	▨	▨	▨	▨	▨	▨
	Variance	▨	▨	▨	▨	▨	▨
Height	Correlation	▨	▨	▨	▨	▨	▨
	SD	▨	▨	▨	▨	▨	▨
	Slope	▨	▨	▨	▨	▨	▩

In our test and before generating the attributes, the aerial photographs (already orthorectified) were registered to the lidar intensity image using a projective transformation. Following the transformation, the image was resampled to 30cm x 30cm cell size in cases of UNSW and Bathurst, and 50cm x 50cm cell size in cases Fairfield and Memmingen by bilinear interpolation to compensate for the difference in resolution between image and lidar data.

For the implementation of SVMs, the Bioinformatics toolbox in Matlab 7.7 was adopted. Four land cover classes were identified which are: buildings, roads, trees, grass. Experiments were conducted on a PC Windows XP with 2.99 GH, 2GB RAM. Before we could use Matlab for SVMs classification, the image data had to be reshaped into a vector with 32 columns (25 generated attributes, 3 image bands (R, G and B), intensity image, NDVI, DSM and FP-LP) and $n_x * n_y$ rows where n_x and n_y are the dimensions of the data sets.

Since we are working with different kinds of images and extracted attributes, before applying the SVMs to classify the data, pixel values of each input band were linearly scaled between 0 and 1. This step was implemented to avoid attributes with large numeric ranges dominating those with smaller numeric ranges (Hsu et al., 2009).

Finally, the attributes were applied for the SVMs classification as described below in seven separate groups which include those from: Red, Green and Blue bands of the aerial image; Intensity image or IR image in the case of the Memmingen data; DSM; FP-LP and the Total group of attributes as shown in table 3. The three image bands (RGB) and the NDVI were considered as the primary data source and available in each test.

Table 3: The seven groups of attributes which were used as input for the classification process: Yes and No indicate whether the attribute has been used for the group or not.

Attributes	Red group	Green group	Blue group	Intensity/IR group	DSM group	FP-LP group	Total group
RGB bands	Yes	Yes	Yes	Yes	Yes	Yes	Attributes from all groups (32 non-repeated attributes) which include: 25 uncorrelated feature attributes in table 3; RGB bands; Intensity/IR image; DSM; FP-LP; and NDVI)
Intensity	No	No	No	Yes	No	No	
Strength	Yes	Yes	Yes	Yes	Yes	Yes	
Homogeneity	Yes	Yes	Yes	Yes	Yes	Yes	
Entropy	Yes	Yes	Yes	Yes	Yes	Yes	
GLCM_mean	Yes	Yes	Yes	Yes	Yes	Yes	
NDVI	Yes	Yes	Yes	Yes	Yes	Yes	
DSM	No	No	No	No	Yes	No	
FP-LP	No	No	No	No	No	Yes	
Slope	No	No	No	No	No	Yes	

5. METHODOLOGY

The filtering process was implemented in several stages as shown in Figure 2.

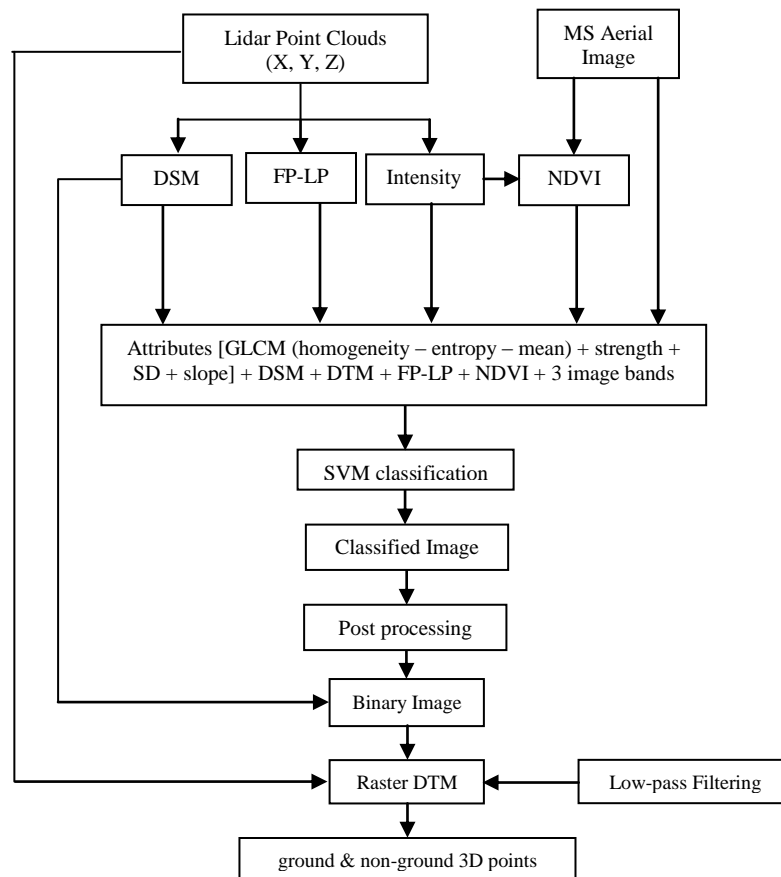


Figure 2: The work flow for filtering of lidar data by data fusion based on SVMs.

The filtering process comprises three main steps as shown below.

5.1 Support Vector Machines (SVMs) classification

Support Vector Machines (SVMs), as one of the more recent developments in the field of machine learning, have proved reliable and accurate in many pattern classification and nonlinear regression tasks and have become a first choice algorithm for many remote sensing users (Van der Linden et al., 2009). SVMs are based on the principles of statistical learning theory (Vapnik, 1979). Being a non-parametric classifier SVMs are particularly well suited to classifying data of high dimensionality and from multiple sources (Waske and Benediktsson, 2007). SVMs delineate two classes by fitting an optimal separating hyperplane to those training samples that describe the edges of the class distribution. As a consequence they generalize well and often outperform other algorithms in terms of classification accuracies, even when only small training sets are available for the classification of highly dimensional data (Pal and Mather, 2006). Also, the problem of over-fitting during the classification of

highly dimensional feature spaces is controlled through the principle of structural risk minimization. Furthermore, the misclassification errors are minimized by maximizing the margin between the data points and the decision boundary (Vapnik, 1995). Figure 3 demonstrates the basic concept of the SVMs classification, in which m is the distance between $H1$ and $H2$, and H is the optimum separation plane which is defined as:

$$w \cdot x + b = 0 \quad (1)$$

Where x is a point on the hyperplane, w is an n -dimensional vector perpendicular to the hyperplane, and b is the distance of the closest point on the hyperplane to the origin. It can be shown that:

$$w \cdot x_i + b \leq -1, \text{ for class 0} \quad (2)$$

$$w \cdot x_i + b \geq 1, \text{ for class 1} \quad (3)$$

Equations (2) and (3) can be combined into:

$$y_i [(w \cdot x_i) + b] - 1 \geq 0 \quad \forall i \quad (4)$$

The SVM attempts to find a hyperplane, equation (1), with minimum $\|w\|^2$ that is subject to constraint (4).

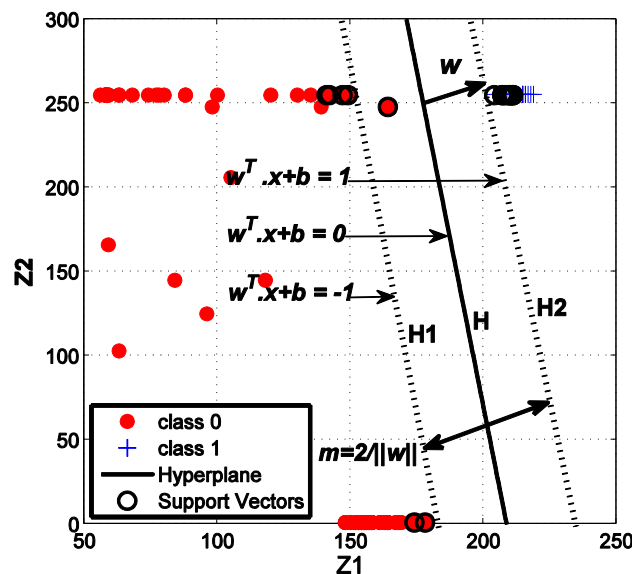


Figure 3: Optimum separation plane in the (Z_1, Z_2) space.

The processing to find the optimum hyperplane is equivalent to solving quadratic programming problems:

$$\begin{aligned} \min (1/2)\|w\|^2 + C \sum_{i=1}^l \xi_i \\ \text{Subject to } y_i[w\phi(x_i) + b] \geq 1 - \xi_i \\ \xi_i \geq 0, i = 1, 2, \dots, l \end{aligned} \quad (5)$$

C is the penalty parameter which controls the edge balance of the error ξ . using the technique of Lagrange multipliers, the optimization problem becomes:

$$\begin{aligned} \min \frac{1}{2} \sum_{i=1}^l \sum_{j=1}^l \alpha_i \alpha_j y_i y_j K(x_i, y_j) - \sum_{i=1}^l \alpha_i \\ \text{Subject to } \sum_{i=1}^l y_i \alpha_i = 0 \\ 0 \leq \alpha_i \leq C, i = 1, 2, \dots, l \end{aligned} \quad (6)$$

Where $K(x_i, y_j) = \phi(x_i) \cdot \phi(y_j)$ is kernel function, the functions used to project the data from input space into feature space. Four kernel functions are available namely: Gaussian, Radius Basis Function (RBF), (Chapelle and Vapnik, 1999); Linear; Polynomial; and Sigmoid (Quadratic). In remote sensing applications the Gaussian radial basis function (RBF) kernel has proved to be effective with reasonable processing times (Van der Linden et al., 2009). A detailed description of SVMs is given by Vapnik (2000).

The sequential minimal optimization (SMO) algorithm (Platt, 1999), with a faster speed and a much smaller memory requirement has been used for our experiments to find the separating hyperplane. In order to solve for the binary classification problem that exists with the SVMs and to handle the multi-class problems in remote sensing and lidar data, two approaches are commonly used:

- the One-Against-All (1AA), which involves training a set of binary classifiers to individually separate each class from the rest;
- One-Against-One (1A1) techniques, which involve training a classifier for each pair of classes resulting in $N(N-1)/2$ classifiers where N is the number of classes. When applied to a data set, each classification gives one vote to the winning class and the point is labelled with the class having most votes.

Anthony et al. (2007) have reported that the resulting classification accuracy from 1AA is not significantly different from 1A1 approach and the choice of technique adopted is based on personal preference and the nature of the used data. Based on these facts and since the 1A1 technique results in a larger number of binary SVMs (a minimum of 6 SVMs are required to classify the image into 4 classes) and then in subsequently intensive computations, the 1AA technique was used for our experiments.

5.1.1 Model selection for support vector machines

Two parameters should be specified while using RBF kernels: C (the penalty parameter that controls the trade-off between the maximization of the margin between the training data

vectors and the decision boundary plus the penalization of training errors) and γ (the width of the kernel function). The problem is that there is no rule for the selection of the kernel's parameters and it is not known beforehand which C and γ are the best for the current problem (Lin and Lin, 2003). Both parameters C and γ depend on the data range and distribution and they differ from one classification problem to another (Van der Linden et al., 2009). As a result there are an infinite number of possible pairs of parameters that could be taken into consideration.

In order to estimate these values and to avoid making exhaustive parameter searches by approximations or heuristics, we used a grid-search on C and γ using a 10-fold cross-validation. The cross-validation procedure can prevent the overfitting problem and results in better accuracy (Hsu et al., 2009). Basically pairs of (C, γ) were tested and the one with the best cross-validation accuracy was picked. First we applied a coarse grid with ranges of values of $[0.001, 0.01, 1, \dots, 10\ 000]$ for both C and γ . Then we applied a finer grid search in the neighbourhood of the best C and γ , obtained from the coarse grid, with ranges of values $[(C \text{ or } \gamma)-10, (C \text{ or } \gamma) +10]$ and with interval of 0.01 to obtain a better cross-validation. Once C and γ have been specified, they were used with the entire training set, to construct the optimal hyperplane. Table 4 shows the obtained C and γ using the seven groups of attributes for the four test areas.

Table 4: C and γ obtained for the four test areas using the seven groups of attributes.

Group	No.	UNSW		Bathurst		Fairfield		Memmingen	
		γ	C	γ	C	γ	C	γ	C
R	8	0.114	8.650	0.076	8.650	0.01	0.015	12.975	748.183
G	8	0.076	19.462	0.051	8.650	0.015	3.844	19.462	1.139
B	8	0.076	12.975	0.034	8.650	0.01	9.853	1.139	98.526
Intensity	9	0.008	8.650	0.01	2.563	0.01	0.384	5.767	2.563
DSM	9	0.051	8.650	0.01	3.844	0.015	8.650	0.506	12.975
FP-LP	10	0.225	8.650	0.034	8.650	0.01	0.01	0.506	8.650
Total	32	0.01	0.577	0.01	0.759	0.01	0.01	0.1	5.767

Figure 4 (a) is a typical example derived in this study showing the classification results for the UNSW test area using the Total group of attributes.

5.2 Generation of the binary image

A binary image was then generated by converting the digital numbers of roads and grass in the final classified image to one, while the digital numbers of buildings and trees were converted to zeros as shown in figure 4 (b). Then all DSM's pixels which correspond to a pixel value of one in the binary image were interpolated into a grid DTM and resampled to the pixels size of the corresponding aerial image. The interpolated DTM was then low-pass filtered, to remove low vegetation and to compensate for the miss-classification errors at edges of buildings and trees. Figure 4 (d) shows the smoothed DTM.

5.3 Filtering of the 3D lidar point clouds

After that the original 3D lidar point clouds was compared against the smoothed DTMs using a threshold of 30 cm (two times the expected accuracy of the lidar system). The original lidar point was labeled as ground if the difference in height between it and the corresponding pixel in the smoothed DTM is less than or equal to the predefined threshold (30cm), otherwise it was labeled as non-ground. This results is two groups of 3D lidar points, one representing the ground and the other, the building and trees. Figure 4 shows the processing results for UNSW test area.

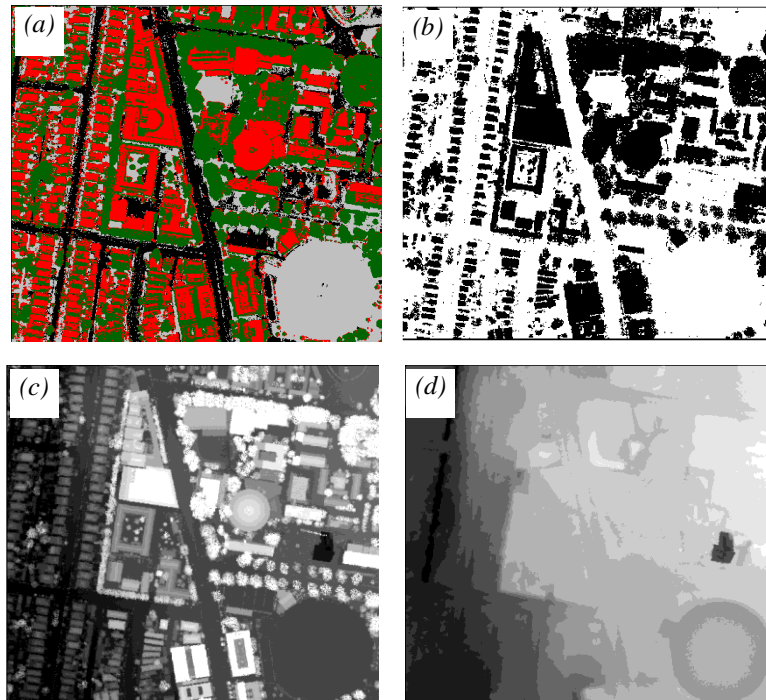


Figure 4: (a) the classified image by SVMs; (b) the produced binary image; (c) DSM; (d) the low-pass filtered DTM.

6. RESULTS AND DISCUSSION

To evaluate the performance of the adopted method for filtering of lidar data, the results were quantitatively and qualitatively checked.

6.1 Quantitative check of the filtering results

There are two basic errors in filtering of lidar data. One is the classification of non-ground measurements as ground points or commission errors, and the other is the assignment of ground points as non-ground measurements or omission errors (Congalton, 1991) as shown in Table 5. All filtering methods are subject to these two types of errors in various degrees. To

evaluate the performance of filtering techniques, these errors should be examined as follows, based on the parameters in Table 5.

Table 5: Definition of omission and commission errors.

	ground	non-ground	
ground	a	b (omission error)	$e = a + b$
non-ground	c (commission error)	d	$f = c + d$
	$g = a + c$	$h = b + d$	$n = a + b + c + d$

$$\text{Percentage of omission errors: } b / e * 100\% \quad (7)$$

$$\text{Percentage of commission errors: } c / f * 100\% \quad (8)$$

$$\text{Percentage of total errors: } (b + c) / n * 100\% \quad (9)$$

First, the reference data was generated by manually filtering the four data sets. In this manual filtering, the original lidar point clouds were overlaid on the ortho image and classified visually as either ground or non-ground features. Then, the SVMs based filtered lidar data was compared against the manually filtered data for the four data sets and omission, commission and total errors were computed and plotted as shown in figure 5. This figure shows that using the Total group of attributes resulted in the most accurate filtering results and reduced the three types of errors to about 1.5%, 7% and 4% for omission, commission and total errors respectively. FP-LP group performed almost as well as the Total group in terms of omission errors, while Intensity group of attributes performed almost as well as the Total group in terms of commission errors. Red, Green and Blue groups performed the worst and almost equal in terms of omission errors, while the DSM group performed the worst in terms of commission errors.

Larger commission errors mean more objects are retained and may decrease the accuracy of the automatic filtering results. However, commission errors are easier to detect and remove through a visual inspection process than omission errors (Sithole and Vosselman, 2003). The most important point to note is that all types of errors using one group of attributes are very consistent for all test areas. This indicates that the SVM method of filtering is robust for different landscape types.

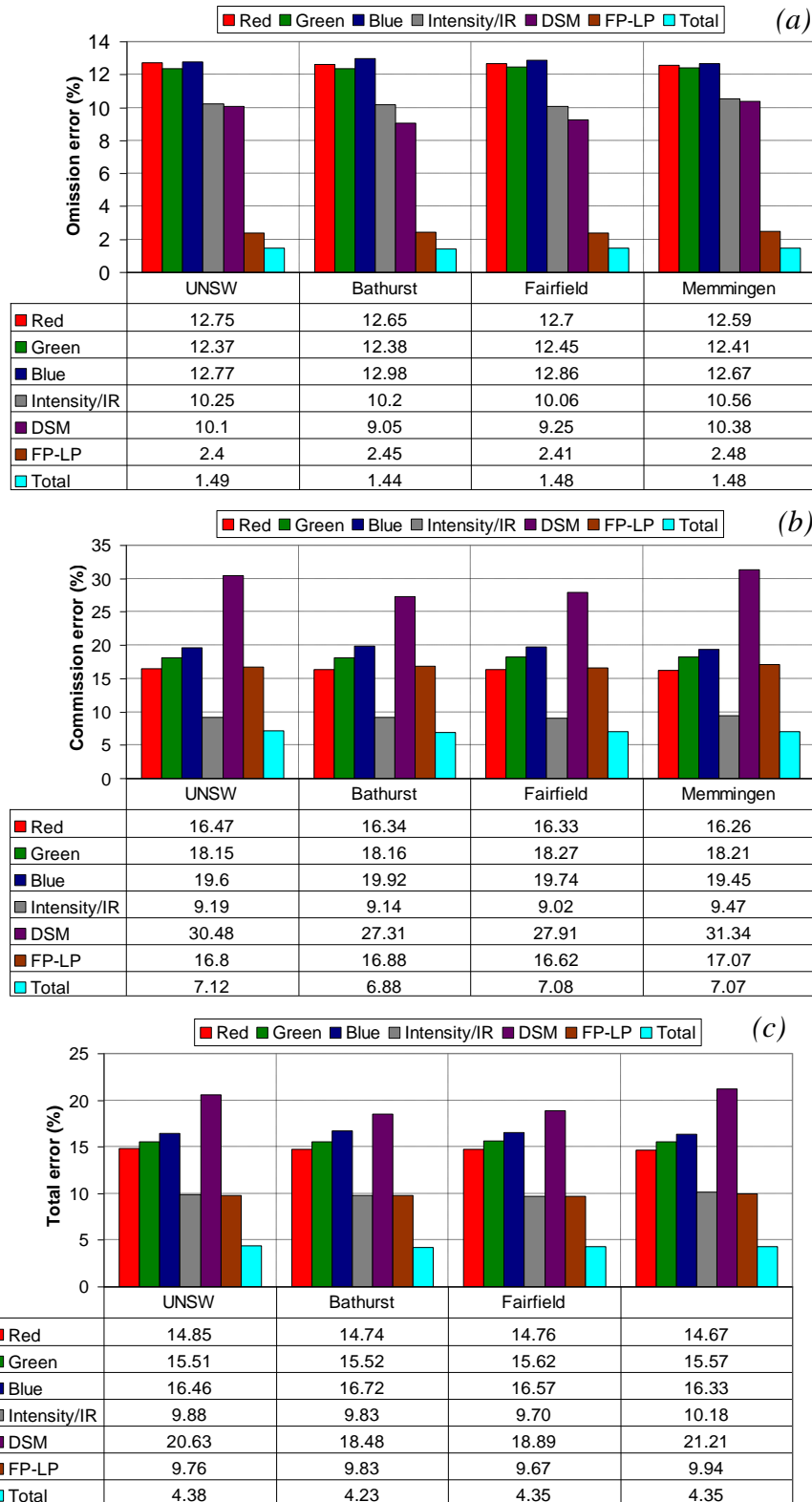


Figure 5: Error comparison of the seven groups of attributes based on filtering using SVM for the four test areas. (a) omission errors, (b) commission errors, and (c) total errors.

6.2 Qualitative check of the filtering results

Another aspect of interests is where the omission and commission errors occur. Most errors occur at the edges of buildings and trees. A possible reason for this could be the effect of between-class variance on the edge pixels which caused many of these pixels to be placed in an incorrect category during the SVM classification process. Also, the errors in the image to lidar geographic registration, of course, will have a negative impact on the produced filtering accuracy. Figure 6 is a typical example of the error distribution map in case of UNSW test area.

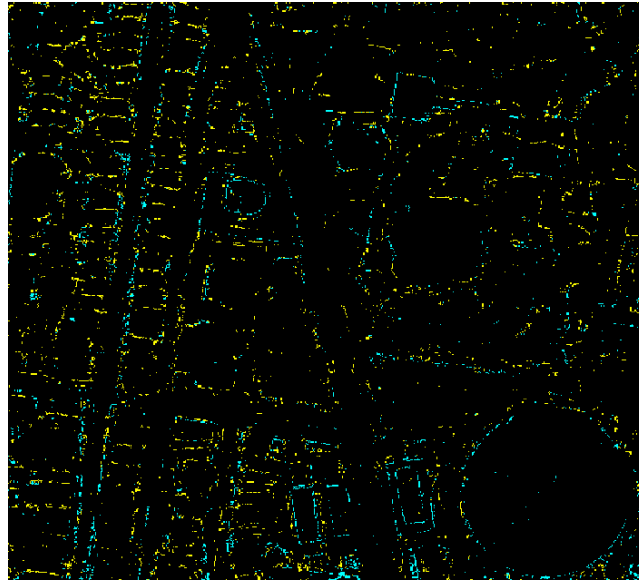


Figure 6: Evaluation of the filtering results for the UNSW dataset using the Total group of attributes. Black: correct terrain pixels; cyan: omission errors; yellow: commission errors.

7. CONCLUSION

A method for filtering of lidar point clouds based on the fusion of lidar, multispectral aerial images and 25 auxiliary attributes based on SVM classification was presented for 4 test areas in different urban environments, based on lidar data derived from 3 different sensors and different vegetation types. The resulted errors ranged from 2.4-12.98%, 9.02-31.34%, 4.23-21.21% for omission, commission and Total errors respectively, but the best results were obtained when the Total group of attributes were used, being 1.5%, 7% and 4% for omission, commission and total errors respectively.

An investigation into the relative importance of the input data showed the relative importance of FP-LP group for reducing omission errors, and the Intensity group for reducing commission errors. Red, Green and Blue groups performed the worst and almost equal in terms of omission errors, while the DSM group performed the worst in terms of commission errors.

Compared with other methods, this technique is simple and requires no work tuning parameters except for C and γ . Also, SVMs based filtering of lidar data effectively removes most of the non-ground points especially those on low vegetation. Moreover, SVMs have the potential to solve sparse sampling, non-linear, high-dimensional data and global optimum problems. As future work, we believe that with more work on enhancing the proposed technique, the scheme can form a new framework for automatic classification of the original lidar point clouds into terrain, low vegetation, trees, buildings and human-made objects.

REFERENCES

- Abo Akel, N., Zilberstein, O. and Doytsher, Y., 2004. A Robust Method Used with Orthogonal Polynomials and Road Network for Automatic Terrain Surface Extraction from LIDAR Data in Urban Areas. *International Archives of Photogrammetry, Remote Sensing and Spatial Information Science*, Vol. 35, ISPRS 274-279.
- Anthony, G., Gregg, H., Tshilidzi M., 2007. Image Classification Using SVMs: One-against-One Vs One-against-All. In: *Proc. 28th Asian Conference on Remote Sensing ARCS, Learning (cs.LG); Artificial Intelligence (cs.AI); Computer Vision and Pattern Recognition (cs.CV)*, Kuala Lumpur, Malaysia, 12-16 November 2007.
- Axelsson, P., 2000. DEM Generation from Laser Scanner Data Using Adaptive TIN Models. *International Archives of Photogrammetry and Remote Sensing*, XXXIII, Part B3:85–92.
- Bartels M. and Wei H., 2006. Towards DTM Generation from LIDAR Data in Hilly Terrain Using Wavelets, 4th *International Workshop on Pattern Recognition in Remote Sensing in conjunction with the 18th International Conference on Pattern Recognition 2006*, I:33-36 (2006)
- Chapelle, O., Vapnik, V., 1999. Model Selection for Support Vector Machines. In: *Proc. Neural Information Processing Systems (NIPS) Conference*, Denver, Colorado, USA, 29 November – 4 December 1999. pp.230-236.
- Clausi, D. A., 2002. An analysis of co-occurrence texture statistics as a function of grey-level quantization. *Canadian Journal of Remote Sensing*, **28**, pp. 45–62.
- Congalton, R.G., 1991. A review of assessing the accuracy of classifications of remotely sensed data. *Remote Sensing of Environment*, 37(1):35–46.
- Elmqvist, M., 2002. Ground Surface Estimation from Airborne Laser Scanner Data using Active Shape Models. *ISPRS Commission III Symposium, Photogrammetric and Computer Vision*, Graz, Austria, pp. 114–109.
- Förstner, W., Gülch, E., 1987. A fast operator for detection and precise location of distinct points, Corners and Centres of Circular Features. *International Archives of Photogrammetry, Remote Sensing and Spatial Information Sciences*, 281–305.
- Gianfranco F., and Carla N., 2007. Adaptive Filtering Of Aerial Laser Scanning Data. *ISPRS Workshop on Laser Scanning 2007*, Espoo, Finland, September 12-14, 2007, pp. 173-177.
- Haralick, R.M., 1979. Statistical and structural approaches to texture. *Proceedings of the IEEE*, **67**, pp. 786–804
- Haugerud, R.A., and Harding, D.J., 2001. Some Algorithms for Virtual Deforestation

- (VDF) of LIDAR Topographic Survey Data. *International Archives of Photogrammetry and Remote Sensing*, XXXIV, Part 3/W4:211–218.
- Hsu, C.W., Chang, C.C., Lin, C.J., 2009. *A Practical Guide to Support Vector Classification*. Department of Computer Science, National Taiwan University, <http://www.csie.ntu.edu.tw/~cjlin/papers/guide/guide.pdf> (Accessed July 23, 2009).
- Kraus K. and Pfeifer N., 1998. Determination of Terrain Models in Wooded Areas with Airborne Laser Scanner Data. *ISPRS Journal of Photogrammetry and Remote Sensing*, Vol. 53 pp193-203.
- Lin, H.T., C.J., Lin, 2003. A study on sigmoid kernels for SVM and the training of non-PSD kernels by SMO-type methods. *Technical report*, Department of Computer Science, National Taiwan University.
- Okagawa, M., 2001. Algorithm of Multiple Filter to Extract DSM from LIDAR Data. *2001 ESRI International User Conference*, Kraus, K., and N. Pfeifer, 1998. Determination of terrain models in wood areas with airborne laser scanner data, *ISPRS Journal of Photogrammetry & Remote Sensing*, 53(4):193–203.
- Pal, M., Mather, P.M., 2006. Some issues in the classification of DAIS hyperspectral data. *International Journal of Remote Sensing* 27(14), 2895-2916.
- Passini, R. and Jacobsen, B.D., 2002. Filtering of Digital Elevation Models. Proceedings of the ASPRS 2002 Annual Convention, 19–26 April, Washington DC (*American Society for Photogrammetry and Remote Sensing*, Bethesda, Maryland), 9 p., unpaginated CD-ROM.
- Platt, J., 1999. *Fast training of support vector machines using sequential minimal optimization*. In: B. Schölkopf, C. J. C. Burges, and A. J. Smola (Eds.), *Advances in Kernel Methods - Support Vector Learning*, Cambridge, MA.: MIT Press, pp.185-208.
- Sithole, G. and vosselman, G., 2003. Comparison of filtering algorithms. In *Proceedings of the ISPRS working group WG III/3 workshop on 3-D reconstruction from airborne laserscanner and InSAR data- XXXIV-3/W13*, 8-10 October 2003, Dresden, Germany, pp. 71–78.
- Van der Linden, S., Rabe, A., Okujeni, A., Hostert, P., 2009. *Image SVM classification, Application Manual: imageSVM version 2.0*. Humboldt-Universität zu Berlin, Germany.
- Vapnik, V., 1979. *Estimation of Dependences Based on Empirical Data* [in Russian]. Nauka, Moscow, 1979. (English translation: Springer Verlag, New York, 1982).
- Vapnik, V., 1995. *The Nature of Statistical Learning Theory*. NY: Springer-Verlag, New York.
- Vapnik, V., 2000. *The Nature of Statistical Learning Theory*, Springer, New York, (chapter 8).
- Vosselman, G., 2000. Slope Based Filtering of Laser Altimetry Data. *International Archives of Photogrammetry and Remote Sensing*, XXXIII, Part B4:958–964.
- Wack, R., Wimmer, A., 2002. Digital Terrain Models from Airborne Laser Scanner Data – A Grid Based Approach. *IAPRS*, Vol. XXXIV Part 3B. *ISPRS Commission III*, Symposium. September 9-13, Graz, Austria. Pp. 293-296.
- Waske, B., Benediktsson, J.A., 2007. Fusion of Support Vector Machines for Classification of Multisensor Data. *IEEE Transactions on Geoscience and Remote Sensing* 45(12-

1), December 2007.

- Whitman, D., K. Zhang, S.P. Leatherman, and W. Robertson, 2003. Airborne Laser Topographic Mapping: Application to Hurricane Storm Surge Hazards. *Earth Sciences in the Cities* (G. Heiken, R. Fakundiny, and J. Sutter, editors), American Geophysical Union, Washington DC, pp. 363–376.
- Zhang, K. and Whitman, D., 2003. Comparison of Three Algorithms for Filtering Airborne Lidar Data. *Photogrammetric Engineering & Remote Sensing*, Vol. 71, No. 3, March 2005, pp. 313–324.
- Zhang, K.Q., S.C. Chen, D. Whitman, M.L. Shyu, J.H. Yan, and C.C. Zhang, 2003. A Progressive Morphological Filter for Removing Non-ground Measurements From Airborne LIDAR Data. *IEEE Transactions on Geoscience and Remote Sensing*, 41 (4): 872–882.

BIOGRAPHICAL NOTES

Mahmoud Salah received his B.Sc. in Surveying Engineering in 1999. In 2004 he received the M.Sc. in Surveying Engineering too. He is currently a PhD visiting fellow at the School of Surveying and Spatial Information Systems, The University of New South Wales, Sydney, Australia while he is an assistant lecturer and PhD candidate at Benha University, Cairo, Egypt. His main fields of interest are image processing and GIS.

Prof. John Trinder graduated from UNSW with a BSurv, MSc at ITC in The Netherlands, and PhD from UNSW. He was employed at the School of Surveying and SIS at University of NSW from 1965 to 1999, progressing to the position of Professor in 1991 and Head of School from 1990-1999. He is currently Emeritus Professor in that School. John has undertaken teaching and research at UNSW for about 40 years, specializing in a range of topics in spatial information, and has published more than 150 scientific papers in journals and conference proceedings. He was President of the International Society for Photogrammetry and Remote Sensing (ISPRS) from 2000-2004.

CONTACTS

Mr. Mahmoud Salah
Prof. John C. Trinder
School of Surveying and Spatial Information Systems, The University of New South Wales
UNSW Kensington Campus
Sydney NSW 2052 Australia
AUSTRALIA
Tel. + 61 2 938 54197
Fax + 61 2 9313 7493
Email: (m.gomah; j.trinder)@unsw.edu.au
Web site: http://www.gmat.unsw.edu.au/staff/vis_ac/trinder.htm